

Properties of Alkali Metal Atoms Deposited on a MgO Surface: A Systematic Experimental and Theoretical Study

Emanuele Finazzi,^[a] Cristiana Di Valentin,^[a] Gianfranco Pacchioni,^{*[a]} Mario Chiesa,^[b] Elio Giamello,^[b] Hongjun Gao,^[c] Jichun Lian,^[d] Thomas Risse,^[d] and Hans-Joachim Freund^[d]

Abstract: The adsorption of small amounts of alkali metal atoms (Li, Na, K, Rb, and Cs) on the surface of MgO powders and thin films has been studied by means of EPR spectroscopy and DFT calculations. From a comparison of the measured and computed g values and hyperfine coupling constants (hfccs), a tentative assignment of the preferred adsorption sites is proposed. All atoms bind preferentially to surface oxide anions, but the location of these anions differs as a function of the deposition temperature and alkali metal. Lithium forms relatively strong

bonds with MgO and can be stabilized at low temperatures on terrace sites. Potassium interacts very weakly with MgO and is stabilized only at specific sites, such as at reverse corners where it can interact simultaneously with three surface oxygen atoms (rubidium and cesium presumably behave in the same way). Sodium forms bonds of in-

termediate strength and could, in principle, populate more than a single site when deposited at room temperature. In all cases, large deviations of the hfccs from the gas-phase values are observed. These reductions in the hfccs are due to polarization effects and are not connected to ionization of the alkali metal, which would lead to the formation of an adsorbed cation and a trapped electron. In this respect, hydrogen atoms behave completely differently. Under similar conditions, they form (H⁺)(e⁻) pairs. The reasons for this different behavior are discussed.

Keywords: adsorption • alkali metals • density functional calculations • EPR spectroscopy • magnesium oxide

Introduction

The interaction of alkali metal atoms with oxide materials and their surfaces is relevant to a wide number of problems and applications. Alkali metals are usually added to inorgan-

ic oxides to modify the electrical and conducting properties of the material. In some cases, such as in tungsten bronzes, this may turn a wide-gap insulating oxide into a material with metallic conductivity. The addition of alkali metals to layered materials is essential for the preparation of ionic conductors and new generations of batteries. Doping with alkali metals can also result in charge imbalance within a material, with the creation of vacancies or changes in the valence state of other atoms, which leads to new chemical properties. A classical case is that of lithium-doped MgO in which the presence of monovalent lithium ions, which replace the divalent magnesium ions in the crystal structure, results in the formation of O⁻ radicals that exhibit a special reactivity, for example, in methane coupling reactions.^[1]

For all of these reasons, the interaction of alkali metal atoms with the surface of an oxide is also of general interest to understand the mechanisms of stabilization and diffusion of the alkali species in the bulk of the material. An oxide that has been investigated in some detail in this context is MgO, a prototype of ionic oxides with a simple crystal structure and a rather well-defined surface morphology.^[2–5] Aside from the general motivations listed above, there are other

[a] E. Finazzi, Dr. C. Di Valentin, Prof. G. Pacchioni
Dipartimento di Scienza dei Materiali, Università di Milano-Bicocca
Via R. Cozzi 53, 20125 Milano (Italy)
Fax: (39) 026-448-5400
E-mail: gianfranco.pacchioni@unimib.it

[b] Dr. M. Chiesa, Prof. E. Giamello
Dipartimento di Chimica IFM and NIS Centre of Excellence
Università di Torino, Via P. Giuria 7, 10125 Torino (Italy)

[c] Prof. H. J. Gao
Beijing National Laboratory for Condensed Matter Physics
Institute of Physics, Chinese Academy of Sciences
P.O. Box 603, 100080 Beijing (China)

[d] J. Lian, Dr. T. Risse, Prof. H.-J. Freund
Fritz-Haber-Institut der MPG, Department of Chemical Physics
Faradayweg 4–6, 14195 Berlin (Germany)

Supporting information for this article is available on the WWW under <http://www.chemeurj.org/> or from the author.

reasons why alkali metal deposition on oxide surfaces, and on MgO in particular, is important. First of all, by depositing alkali metal atoms on MgO one can selectively dope the surface and generate new electron-rich sites that exhibit a special reactivity towards adsorbed species. On the other hand, when the properties of the deposited atomic species are monitored with sophisticated techniques, such as EPR spectroscopy, one can learn about the essence of the metal-oxide bonding interaction, the nature of the surface adsorption sites, and indirectly about the abundance of these sites and the morphology of the surface. In this respect, alkali metal adatoms are excellent probes of local adsorption sites and their environment. In addition, if alkali metals are adsorbed on different oxides with similar crystal structures, for example, MgO, CaO, and SrO, it is possible to titrate the surface basicity of the oxide in a very accurate way.^[2,3] In fact, changes in the adsorption properties of the alkali metal adatom provide indirect, but detailed, information about the tendency of surface anions to donate charge to an adsorbed species. Last, but not least, alkali metals on MgO surfaces represent an excellent system to test the validity of theoretical methods and models to interpret and predict the properties of adsorbed atoms (in particular to reproduce observable EPR properties, such as *g* factors and hyperfine coupling constants (hfccs), in both isotropic, a_{iso} , and dipolar, *B* tensor, forms).^[2,4]

The aim of this study was to systematically investigate the properties of alkali metal atoms deposited on a MgO surface to extend previous experiments by looking at the behavior of the heavier members of the group and exploring the interaction at various surface sites with respect to their site-specificity. For the sake of completeness we will also consider the behavior of hydrogen atoms adsorbed on the same surface because hydrogen may be regarded as the "first alkali metal".^[6] The behavior of both alkali metal atoms^[2-5,7] and hydrogen^[8-14] adsorbed on MgO has been investigated previously, but a direct comparison has never been made. In addition, a comprehensive picture is often hampered by the complex morphology of the polycrystalline MgO surface used. In this paper we provide a unified picture by combining published data with new results. In particular, we report new experiments that characterize cesium atoms, which complete the data for the alkali-metal series. On the theoretical side we report a new set of calculations based on a more sophisticated approach than has been used in the past (the shell model). Furthermore, some new adsorption sites (e.g., the reverse edge), metal atoms (e.g., lithium), and measurable properties (e.g., *g* factors) are considered here for the first time.

It has previously been shown that full ionization of the alkali metal takes place only at very few sites that can be saturated at very low metal coverage.^[4] These minority sites have been tentatively identified as empty F^{2+} centers, that is, strongly electron-deficient oxygen vacancies. After saturation of all of the " F^{2+} " centers, slightly larger amounts of alkali metal lead to EPR signals characteristic of alkali metal atoms stabilized as monomeric entities at specific sur-

face sites.^[2,4] At these sites the atoms are often stable at room temperature or above, which means the diffusion barriers for these atoms are very high. An additional increase in the amount of deposited metal results in the formation of tiny clusters and small aggregates.^[5] Theoretical calculations and EPR measurements on ^{17}O -enriched MgO samples have demonstrated that the alkali metal atoms are preferentially bound to oxide anions and stabilized at specific sites at which the *ns* valence electron is strongly polarized.^[2] A comparison of theoretical and experimental results has shown that the metal atom remains basically neutral, despite very large changes in the measured hfccs.^[2] Very similar conclusions have been reached for the deposition of gold adatoms on MgO thin films.^[15]

The behavior of atomic hydrogen is very different and has been discussed in detail in a series of papers.^[8-14] Herein, some account of the reactivity of hydrogen atoms is given, which will be restricted to the factors that distinguish them from the Group Ia metals. Finally, the trends in the chemical bonding and EPR properties of the alkali metal atoms going from the lighter (lithium) to the heavier (cesium) atoms are discussed.

Results and Discussion

EPR data: Experimentally measured values of the *g* factor and isotropic hfccs of free (gas phase) alkali and hydrogen atoms are reported in Table 1. For comparison, the same

Table 1. Experimental and theoretical EPR parameters for the free atomic values of the alkali atoms.

	$\lambda_{\text{s-o}}$ [eV]	Exp.		DFT	
		<i>g</i>	a_{iso} [G]	<i>g</i>	a_{iso} [G]
^1H	–	2.00230	506.7	2.00228	471.3
^7Li	2.72×10^{-5}	2.00231	143.4	2.00230	155.5
^{23}Na	1.41×10^{-3}	2.00231	316.1	2.00234	334.7
^{39}K	4.75×10^{-3}	2.00231	82.4	2.00238	83.9
^{85}Rb	1.95×10^{-2}	2.00241	361.1	–	–
^{133}Cs	4.55×10^{-2}	2.00258	819.8	–	–

quantities have been calculated theoretically by using the basis sets described in the Experimental Section. Note that there is quite a good agreement between theory and experiment. The *g* factors are reproduced quantitatively up to the fourth decimal digit; the hfccs exhibit some deviations in the case of lithium (+8%) and sodium (+6%), whereas the error on potassium is negligible (+2%).

The EPR properties of the alkali metal atoms change substantially when they are deposited on MgO. This is true in particular for the isotropic component of the hfcc (Table 2). In general, we observe a strong reduction in the a_{iso} values of between 45 and 52% of the free atomic value for sodium, potassium, rubidium, and cesium. For these atoms the experiments were performed with polycrystalline MgO and the alkali deposition was carried out in a vacuum at room

Table 2. Experimental values of the EPR parameters for alkali atoms adsorbed on the surface of MgO powders.

M	g_{\parallel}	g_{\perp}	$a_{\text{iso}}(\text{M})$ [G]	B [G]	$a_{\text{iso}}(^{17}\text{O})$ [G]	$a_{\text{iso}}(^{25}\text{Mg})$ [G]	Ref.
^1H	2.0013 ± 0.0001	1.9994 ± 0.0001	-1.2 ± 0.1 (0%)	-0.7	-50.2 ± 0.5	-10.9 ± 0.1 -27.3 ± 0.1 -60.3 ± 0.1	[13,16]
$^7\text{Li}^{\text{[a]}}$	2.003 ± 0.001	2.000 ± 0.001	74 ± 0.5 (52%)	0	-	-	[7]
^{23}Na	2.001 ± 0.001	2.000 ± 0.001	140.8 ± 0.5 (45%)	0.8	-2.0 ± 0.5	-	[3]
^{39}K	2.000 ± 0.001	1.999 ± 0.001	41.4 ± 0.5 (50%)	0.2	-2.8 ± 0.1	-	[2]
^{85}Rb	1.996 ± 0.001	1.995 ± 0.001	184.0 ± 1.0 (51%)	2.0	-	-	[5]
^{133}Cs	1.995 ± 0.001	1.993 ± 0.001	426.4 ± 0.5 (52%)	0.1	-	-	this work

[a] UHV experiments on MgO thin films.

temperature. Lithium atoms were deposited on a thin MgO film (20 monolayers) at 35 K in ultra-high vacuum (UHV).^[7] Clearly, the two temperatures at which the EPR measurements were carried out result in different thermal behavior. On the polycrystalline samples the deposited atoms possess enough thermal energy to diffuse across the surface until they are trapped at specific binding sites. On thin films atoms remain where they land, that is, on the flat (100) terraces that represent the majority of sites in the sample. The effect is similar and the reduction in the a_{iso} value is about 50% (Table 2). The origin of the reduction in a_{iso} has already been discussed for the case of potassium adsorbed on MgO.^[2] It is not related to a delocalization of the spin density to other nuclei at the surface. Rather, it can be interpreted in terms of an intrinsic nephelauxetic effect whereby the ns orbital becomes strongly destabilized by the interaction with the surface oxygen ions. In a similar manner to classical solvation, the resulting species may be regarded as an “expanded atom” and has similarities to a gas-phase excited state. More recently, the same effect was clearly identified for gold atoms deposited on the terrace sites of MgO thin films grown on Mo(100).^[15]

The properties of the smallest “alkali atom”, hydrogen, are markedly different from those of the rest of the members of the group (Table 2). When hydrogen atoms are deposited on polycrystalline MgO, there is a dramatic reduction in the spin density of the hydrogen atom and the hfcc is drastically reduced compared with the free-atom value. Simultaneously, a rather large hyperfine interaction occurs with both the ^{17}O and ^{25}Mg nuclei at the surface, which is different from the alkali metals for which only small ^{17}O and no ^{25}Mg hyperfine interactions are observed (Table 2). Note also that the residual spin density on the hydrogen atom has a negative value, as indirectly assessed from computer simulations of Q-band ENDOR spectra^[16] (note that the negative $a_{\text{iso}}(^{17}\text{O})$ and $a_{\text{iso}}(^{25}\text{Mg})$ values in Table 2 are due to the negative magnetic moment of these nuclei). This is at variance with the cases of the alkali atoms for which positive values are derived from the experiment, in agreement with calcu-

lated values (see below). A negative sign for the hydrogen hyperfine coupling constant, which corresponds to a negative spin density on the nucleus, is expected for ion pairs when the counterion is located at a node of the molecular orbital occupied by the unpaired electron. This fact further confirms the ionization of the electron from the parent hydrogen nucleus and indicates that the resulting

species may be properly described in terms of a $(\text{H}^+)(\text{e}^-)$ ion pair in which the electron plays the role of the anion.

The experimental data recorded for the various alkali metal atoms on MgO (Table 2) refer to the most abundant adsorption site under the conditions of temperature, surface area, and morphology used in the experiment. Except for single crystalline MgO films, it is not possible to infer directly from experiments which sites are decorated by the alkali adatoms unless a combined experimental and theoretical approach is followed. For this reason it is quite useful to compare the measured EPR properties with those derived from ab initio calculations.

DFT results

Terrace sites: We start by considering the adsorption at MgO(100) terrace sites. At these sites the hydrogen atom has a special behavior with respect to adsorption at low-coordinated sites. When hydrogen is adsorbed on a five-coordinated O_{5c} ion, it is ionized, but, in the absence of low-coordinated magnesium cations, the corresponding electron is spread and delocalized over several sites. The situation is clearly unfavorable compared with adsorption on low-coordinated sites and is not expected to be observed experimentally. Note that the computed a_{iso} in this case (Table 3) has a small but positive value in contrast with that determined experimentally (Table 2). This suggests considerable dielectric screening of the electron–nucleus pair, which means that the unpaired electron has a large Bohr radius, a situation that is reminiscent of shallow impurity states in n-type doped Group IV semiconductors.

The situation is different for the alkali metal atoms. The computed binding energy of lithium atoms on terrace sites is relatively large, about 1 eV (note that this is much larger

Table 3. Computed properties of alkali atoms adsorbed on terrace sites of the MgO(100) surface.^[a]

M	D_e [eV]	$r(\text{M}-\text{O})$ [Å]	$a_{\text{iso}}(\text{M}_{\text{ad}})$ [G] ^[b]	B_1 [G]	B_2 [G]	B_3 [G]	g_{\parallel}	g_{\perp}	$a_{\text{iso}}(^{17}\text{O})$ [G]	$a_{\text{iso}}(^{25}\text{Mg})$ [G]
H	0.50	1.01	0.6 (0%)	8.9	-4.5	-4.5	2.00164	2.00079	-64.3	-4.0
Li	1.05	1.83	75.5 (49%)	0.7	-0.3	-0.3	2.00220	2.00105	-10.8	-0.9
Na	0.44	2.38	228.0 (68%)	2.1	-1.0	-1.0	2.00230	2.00095	-12.3	-0.5
K	0.18	2.85	62.7 (75%)	0.5	-0.3	-0.3	2.00251	2.00041	-6.3	-0.4

[a] D_e = adsorption energy; $r(\text{M}-\text{O})$ = shortest M–O distance. [b] The ratio with respect to the free-atom value is given in parentheses.

than the DFT barrier for diffusion, $E_b < 0.4$ eV). Thus, it is expected that lithium atoms will, at least partially, reside on the O_{5c} anions when deposited at low temperatures (experiments were carried out at 35 K, see above). The calculations (Table 3) indicate a reduction of about 50% in the value of $a_{\text{iso}}(\text{Li})$, from 155.5 to 75.5 G, and very small dipolar components, in very good agreement with experimental observations (Table 2). The g tensor exhibits a small deviation from the free-electron value, in particular for the g_{\perp} component, again consistent with experiment. Thus it is likely that the observed EPR signal stems from lithium atoms adsorbed on terrace sites.

Sodium binds more weakly to O_{5c} ions than lithium (0.44 eV; Table 3 and Figure 1). The atom is bigger, its distance from the surface oxygen is greater, and hence the

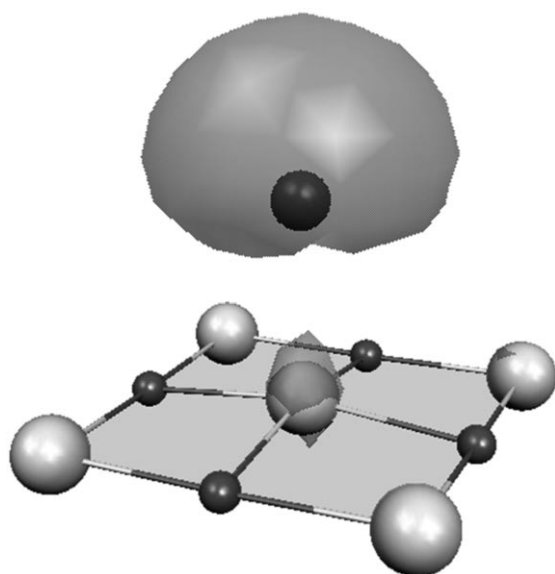


Figure 1. Spin density plot for a sodium atom adsorbed on a terrace site. Only part of the cluster model is shown. Grey atoms: Mg; white atoms: O. The contour corresponds to a density of $0.002 \text{ e bohr}^{-3}$.

overlap with the oxide orbitals is smaller. For all these reasons, the EPR properties of the sodium adatom exhibit a smaller deviation from the free atom than the lithium adatom: $a_{\text{iso}}(\text{Na})$ is 228.0 G, that is, 68% of the value of the free sodium atom. This trend is sustained for potassium, which exhibits an $a_{\text{iso}}(\text{K})$ of 62.7 G, or 75% of the free-atom value. The dipolar component is always negligible. The g tensors of adsorbed sodium and potassium atoms have very similar structures and values to those of lithium (Table 3). In particular, the g_{\parallel} components are close to those of the free atoms (Table 1), whereas smaller deviations are observed for g_{\perp} . This reflects a nonspherical distribution of the spin density

when the atom is adsorbed on the surface. In general, the g tensor seems to be a less sensitive probe of the adsorption properties than the hyperfine coupling constants.

The $a_{\text{iso}}(M_{\text{ad}})$ value for each metal atom seems to inversely correlate with the M–O distance (Table 3). However, if we divide this latter quantity by the atomic van der Waals radius of each alkali atom,^[17] we obtain a constant value of approximately one. Thus, the smaller perturbation of the alkali atom density is not due to the longer M–O distance. Rather, the decrease relative to the free atom in hfccs from lithium to sodium and potassium correlates well with the monotonous decline of the interaction energy. This suggests that the level of distortion of the valence electron cloud is directly related to the strength of the covalent interaction between the 2p levels of the oxygen atom and the ns orbital of the metal.

An additional way to characterize the interactions of the alkali metal atoms with the substrate is to analyze the hyperfine interactions with the ^{17}O ions of the MgO lattice. For lithium, sodium, and potassium, small $a_{\text{iso}}(^{17}\text{O})$ values for their interactions with the O_{5c} surface ions have been calculated. Depending on the alkali metal atom, they range from 6 to 12 G (see Table 3), which indicates a partial transfer of spin density to the substrate anion. In contrast, the interaction with the neighboring magnesium cations is negligible (Table 3). Thus, the analysis of the hyperfine interaction with an ^{17}O -enriched MgO sample can provide compelling evidence of the site at which the alkali atom is bound, provided that the signal in the experimental spectrum is sufficiently intense.

Edge sites: All of the alkali atoms are more strongly bound to the O_{4c} anions of the edge sites than to the O_{5c} anions of the terraces (Table 4 and Figure 2). The binding energies are increased by about 0.2 to 0.3 eV. The interaction energies, however, are rather different for the three alkali metals, whereas lithium is strongly bound (1.34 eV), sodium and potassium atoms form bonds of medium strength. The stronger interactions compared with the terrace example result in shorter M–O bonds and larger reductions in $a_{\text{iso}}(M)$ from the free atomic values. For lithium, the computed a_{iso} value is about 42% of the free atomic value, whereas for sodium and potassium it is about 60 to 70% of the free-atom value. Although for lithium the reduction is too large in relation to the experimentally observed splitting, for the heavier members, the reductions are less than those observed experimentally, which are about 50% (Table 2). The qualitative behav-

Table 4. Computed properties of alkali atoms adsorbed on edge sites of the MgO(100) surface.^[a]

M	D_e [eV]	$r(\text{M}-\text{O})$ [Å]	$a_{\text{iso}}(M_{\text{ad}})$ [G] ^[b]	B_1 [G]	B_2 [G]	B_3 [G]	g_{xx}	g_{yy}	g_{zz}	$a_{\text{iso}}(^{17}\text{O})$ [G]	$a_{\text{iso}}(^{25}\text{Mg})$ [G]
H ^[c]	1.66	0.98	−4.5 (1%)	5.6	−4.0	−1.6	1.99949	2.00027	2.00197	−57.0	−14.8
Li	1.34	1.75	64.9 (42%)	0.5	−0.5	0.0	2.00141	2.00142	2.00215	−20.2	−4.2
Na	0.69	2.23	194.4 (58%)	2.2	−1.1	−1.1	2.00086	2.00124	2.00223	−21.7	−2.1
K	0.51	2.61	56.6 (67%)	0.4	−0.3	−0.1	2.00035	2.00143	2.00233	−16.3	−2.7

[a] D_e = adsorption energy; $r(\text{M}-\text{O})$ = shortest M–O distance. [b] The ratio with respect to the free-atom value is given in parentheses. [c] From ref. [13] (EPR-II basis set on the hydrogen atom).

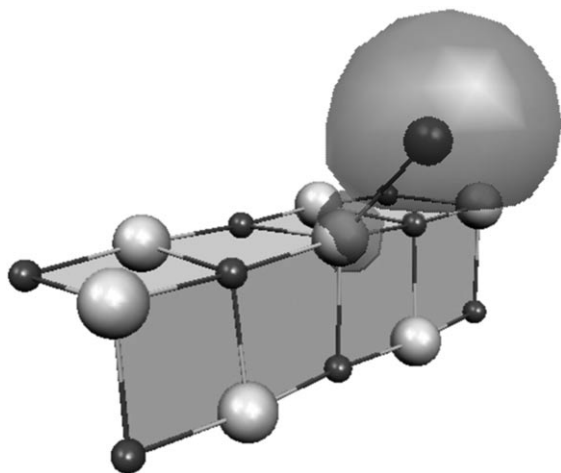


Figure 2. Spin density plot for a sodium atom adsorbed on an edge site. Only part of the cluster model is shown. Grey atoms: Mg; white atoms: O. The contour corresponds to a density of $0.002 \text{ e bohr}^{-3}$.

ior remains unchanged: the spin density on the three atoms is about 0.8, which indicates that the adsorbed alkali atoms are almost neutral.

The hyperfine interaction remains largely isotropic, with negligible dipolar contributions. The increase in metal polarization is accompanied by an increase in the spin density transferred to the oxygen adsorption site. Lithium, sodium, and potassium exhibit $a_{\text{iso}}(^{17}\text{O})$ values of 16 to 22 G (Table 4), about twice as large as those on terrace sites. These values are about ten times larger than those observed experimentally (Table 2). The calculated hfcc may be overestimated, as discussed previously.^[2] However, in combination with the isotropic hfccs of the metal atoms discussed above, the data suggest that the alkali atoms are most likely not adsorbed on edge sites. The coupling with the magnesium ions is slightly larger than on the terraces, which indicates that the electron is a bit more delocalized. Owing to the reduced symmetry, the g matrix is no longer axial, but the three principal g components are only moderately shifted with respect to the free-electron value.

At this point we should comment on the peculiarity of the hydrogen atom. On low-coordinated sites, a spontaneous splitting of hydrogen into an adsorbed proton and a trapped electron occurs. The two entities, (H^+) and (e^-), remain close,^[9,14] but the electron interacts mainly with a Mg_{dc} cation ($a_{\text{iso}} = -14.8 \text{ G}$, which is in good agreement with the experimental value, -10.9 G , Table 2), whereas the hyperfine interaction with the proton is small. Noticeably, the calculated value has a negative sign, in accordance with the experimental value (note also in this case that absolute values are partly overestimated in the calculations). Moreover, the interaction with the oxygen atom of the hydroxy group is considera-

bly stronger. Experiments performed on ^{17}O -enriched MgO samples have an $a_{\text{iso}}(^{17}\text{O})$ value of -50 G (Table 2).^[13] Thus, the electronic structure of hydrogen atoms adsorbed on an edge site of MgO differs completely from that of lithium, sodium, and potassium atoms adsorbed on the same site. Although an almost complete separation of the electron occurs for hydrogen atoms, the alkali atoms must be considered as neutral adsorbed species on the surface.

Reverse edge sites: The reverse edge site is formed at the intersection between two (001) planes (Figure 3). Transmission electron micrographs of MgO powders show that these ex-

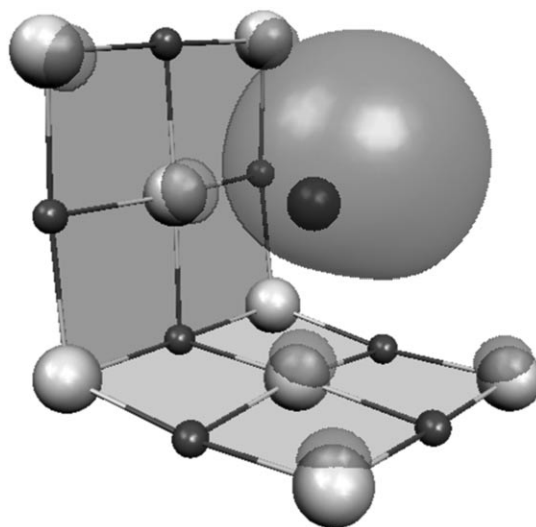


Figure 3. Spin density plot for a sodium atom adsorbed on a reverse edge site. Only part of the cluster model is shown. Grey atoms: Mg; white atoms: O. The contour corresponds to a density of $0.002 \text{ e bohr}^{-3}$.

tended defects are rather abundant.^[13] An atom diffusing across a terrace site has a non-negligible probability of remaining trapped at these sites where it can interact simultaneously with two O_{sc} anions. Thus, a stronger interaction with the surface might be expected. The calculations show that sodium and potassium are more strongly bound than on regular terrace sites (but more weakly than on the previously discussed edge sites, Table 5). On the other hand, the reverse edge provides a strong adsorption site for lithium (1.6 eV) that is stronger than on both previously discussed sites. Not surprisingly, the effect of interacting with two

Table 5. Computed properties of alkali atoms adsorbed on reverse edge sites of the MgO(100) surface.^[a]

M	D_e [eV]	$r(\text{M}-\text{O})$ [Å]	$a_{\text{iso}}(\text{M}_{\text{ad}})$ [G] ^[b]	B_1 [G]	B_2 [G]	B_3 [G]	g_{xx}	g_{yy}	g_{zz}	$a_{\text{iso}}(^{17}\text{O})$ [G]	$a_{\text{iso}}(^{25}\text{Mg})$ [G]
Li	1.65	1.88	40.0 (26%)	0.9	-0.7	-0.2	2.00055	2.00067	2.00106	-9.3	-0.4
Na	0.59	2.36	168.9 (51%)	3.6	-1.8	-1.8	1.99906	1.99961	2.00132	-8.5	-0.2
K	0.29	2.92	52.3 (64%)	0.7	-0.4	-0.3	1.99850	1.99897	2.00168	-3.9	-0.1

[a] D_e = adsorption energy; $r(\text{M}-\text{O})$ = shortest M-O distance. [b] The ratio with respect to the free-atom value is given in parentheses.

oxide anions reinforces the polarization effect of the valence electron cloud so that the reduction in $a_{\text{iso}}(\text{M})$ with respect to the gas phase is enhanced. In particular, ratios of 26, 51, and 64% with respect to the gas phase are found for lithium, sodium, and potassium, respectively. The g values show small deviations from the free-electron values, which increase with the size of the alkali atom. The a_{iso} value computed for lithium (40 G) is clearly inconsistent with that measured experimentally (74 G, Table 2). In contrast, the values obtained for sodium (169 G) and potassium (52 G) are only slightly larger than the experimental ones (141 (Na) and 41 G (K), Table 2). Based on this comparison one cannot exclude the possibility that sodium and potassium atoms are bound to reverse edge sites. Also the $a_{\text{iso}}(\text{O})$ values are comparable and only a few G larger than the experimental values. However, for deposition at room temperature, which was performed herein, the binding energy of potassium is clearly too small to account for the thermal stability at this site, whereas adsorption of sodium cannot be excluded.

Anionic reverse corner sites: A site on the surface of cubic ionic crystals that has recently received considerable attention in the analysis of surface reactivity is the anionic reverse corner (ARC, Figure 4). This site is characterized by the presence of two O_{4c} and one O_{3c} anions that form a triangular unit with a (111) orientation. The possibility of metal atoms binding simultaneously to the three oxide anions results in strong interactions and thermally stable adsorbed species. The binding energy at these sites decreases from 2.4 eV for lithium, to 1.5 eV for sodium, and 1.1 eV in the case of potassium (Table 6). Even the heavy rubidium and cesium atoms, which interact only very weakly with the

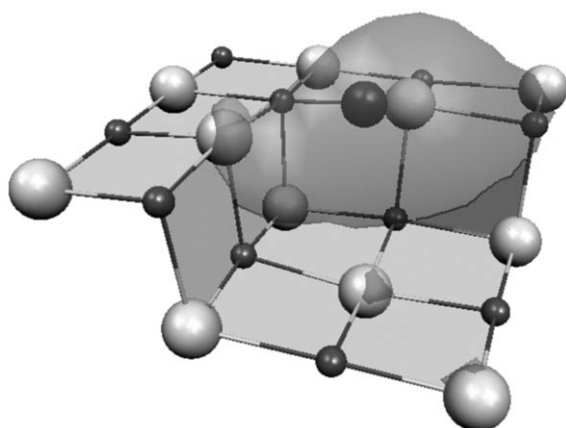


Figure 4. Spin density plot for a sodium atom adsorbed on an anionic reverse corner site. Only part of the cluster model is shown. Grey atoms: Mg; white atoms: O. The contour corresponds to a density of $0.002 \text{ e bohr}^{-3}$.

Table 6. Computed properties of alkali atoms adsorbed on anionic reverse corner (ARC) sites of the MgO -(100) surface.^[a]

M	D_e [eV]	$r(\text{M-O})$ [Å]	$a_{\text{iso}}(\text{M}_{\text{ad}})$ [G] ^[b]	B_1 [G]	B_2 [G]	B_3 [G]	g_{xx}	g_{yy}	g_{zz}	$a_{\text{iso}}(^{17}\text{O})$ [G]	$a_{\text{iso}}(^{25}\text{Mg})$ [G]
Li	2.37	1.93	16.2 (10%)	0.7	-0.6	-0.2	2.00092	2.00155	2.00290	-10.7	-6.9
Na	1.49	2.26	93.2 (28%)	3.9	-2.0	-1.9	2.00041	2.00080	2.00166	-12.1	-4.9
K	1.09	2.62	34.1 (41%)	0.9	-0.5	-0.4	1.99933	1.99976	2.00186	-10.3	-4.3

[a] D_e = adsorption energy; $r(\text{M-O})$ = shortest M-O distance. [b] The ratio with respect to the free-atom value is given in parentheses.

rest of the MgO surface sites, are bound by 0.63 and 0.54 eV, respectively (for the calculations on both rubidium and cesium an effective core potential was used so the values of hfccs could not be determined). Of course, more than the absolute adsorption energies, what is important here are the barriers to diffusion, which are certainly lower. Nevertheless, the adsorption energy provides a simple measure of the stability of a given site. The ARC sites are thus excellent traps for alkali metal atoms diffusing across the surface of polycrystalline oxides and are the sites that are most likely to be populated at room temperature. For these reasons, the EPR properties of alkali metals deposited on this site are of special interest.

The spin density of the alkali atom is strongly distorted, but symmetrically distributed over the two O_{4c} sites (Figure 4). We discuss first sodium and potassium for which experiments on polycrystalline MgO are available (Table 2). The experimental EPR spectra are axial with $g_{\parallel} = 2.001$ and $g_{\perp} = 2.000$ for sodium and $g_{\parallel} = 2.000$ and $g_{\perp} = 1.999$ for potassium (Table 2). The symmetry allows for a splitting of g_{\perp} into g_{xx} and g_{yy} ; experimentally this discrimination may be hampered by limited spectral resolution. In the calculations, the two values of g_{xx} and g_{yy} are indeed very close: 2.0004 and 2.0008 for sodium ($g_{zz} = 2.0017$), and 1.9993 and 1.9998 for potassium ($g_{zz} = 2.0019$; Table 6). The agreement with the experimental data is extremely good.

Theoretically, a huge reduction in $a_{\text{iso}}(\text{M})$ values is observed for these sites, as shown in particular for lithium (10% of the free-atom value) and sodium (28%). Naively one would interpret such a reduction to be a result of charge transfer and conclude the atoms to be metal cations. On the contrary, the calculations clearly show a spin population of about one for all three atoms, hence they are neutral atoms. This is a clear example of the importance of a combined theoretical and experimental approach. A simple-minded comparison of the measured hfccs for the free and supported atoms would lead to an incorrect conclusion about the nature of the adsorbate.

A comparison with the experimental results shows that the measured $a_{\text{iso}}(\text{M})$ for K/MgO (41.4 G) is only slightly larger than the computed one (34.1 G; Table 6). In contrast, for sodium the computed value is greatly underestimated (93.2 versus 140.8 G (exp.)). This suggests that the sodium atoms do not reside on ARC sites, whereas potassium atoms are likely to do so.^[2] This can be understood by considering that the interaction with the MgO surface is stronger for

sodium than for potassium. Although at room temperature potassium is stable only at ARC sites, sodium can be adsorbed on less strongly binding but more abundant sites, such as reverse edges.

Cationic reverse corner sites: Finally, we consider the adsorption of alkali metal atoms on a cationic reverse corner (CRC). This site is the equivalent of the ARC, but with cations and anions interchanged. The site is thus characterized by the presence of three magnesium cations, two Mg_{4c} and one Mg_{5c} . Alkali metals, however, bind preferentially to the oxygen atoms and thus form bonds with the O_{4c} and O_{5c} ions (Figure 5); the coordination is similar to that assumed by the atoms on a monoatomic step. Owing to the shape of the adsorption site, the spin density is strongly polarized towards the reverse corner and is highly asymmetric (Figure 5).

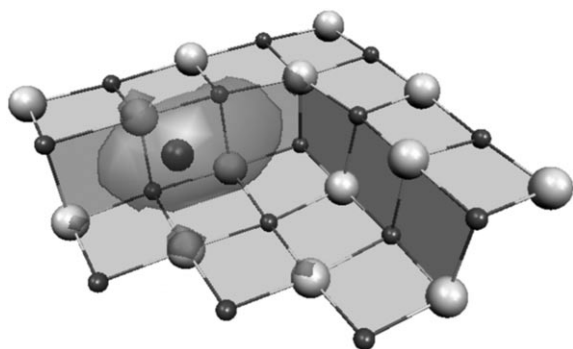


Figure 5. Spin density plot for a sodium atom adsorbed on a CRC site. Only part of the cluster model is shown. Grey atoms: Mg; white atoms: O. The contour corresponds to a density $0.002 \text{ e bohr}^{-3}$.

The reduction in the hyperfine interaction with the metal nucleus, observed for other sites, is also very pronounced on the CRC. For lithium, a_{iso} is reduced to 26.3 G, that is, about 17% of the free-atom value (Table 7). Note that this only corresponds to a partial loss of the valence electron; the spin population on lithium is about 0.5. The dipolar part of the hfcc is negligible. The lithium 2s electron is strongly polarized away from the atom owing to the attraction of the low-coordinated cations at the CRC; this drastically reduces its interaction with the nucleus. For sodium, the effect is

similar, only partly attenuated (Figure 5). Here $a_{\text{iso}}(\text{Na}) = 148.3 \text{ G}$, about 44% of the free-atomic value. The comparison with the case of hydrogen adsorption on the same site is interesting (Table 7). For both hydrogen and lithium we observe a large reduction in a_{iso} (this is only 3 G for hydrogen) and the absence of considerable dipolar contributions. On this basis one could conclude that the two adsorbates have a similar character. However, there are significant differences, as shown by the hyperfine interaction with magnesium surface cations. For hydrogen, the interaction with magnesium is large at 33.0 G, whereas for lithium it is only 11.3 G (Table 7). This is a clear indication that, although for hydrogen the electron has been largely displaced (actually detached) with the formation of a $(\text{H}^+)(\text{e}^-)$ ion pair, this is not the case for lithium, and even less so for sodium and potassium. The alkali metal atoms are strongly polarized and partly ionized, but a consistent fraction of the spin density is still localized near the nucleus.

Although less tightly binding than the ARC, the CRC site is able to trap diffusing metal atoms and bind them rather strongly: lithium 1.64 eV, sodium 0.79 eV, and potassium 0.60 eV (Table 7). This renders the CRC the second strongest binding site considered in this work. This suggests that it could be possible to populate this site with sodium atoms at room temperature. This hypothesis is consistent with the close similarity of the computed $a_{\text{iso}}(\text{Na})$ value for adsorption at this site (148 G) and the measured one (141 G; Table 2). Also, the g values are qualitatively consistent: 1.999–2.001 theory, 2.000–2.001 experiment. Despite the relatively good agreement between the computed and experimental values, these data should be handled with care as the agreement may be fortuitous. Also, considering the relatively large hyperfine interaction with a surface oxygen found for this site, inconsistent with the measurements, the CRC site is less likely to be a trapping site for sodium atoms than, for instance, the reverse edge.

In fact, recent experiments by some of us have clearly shown that the sodium hfcc is monotonically reduced when sodium atoms are deposited on the more basic calcium and strontium oxides.^[3] In particular, the decrease in the hfcc has been found to parallel the increase in the oxide basicity which, in turn, is linked to the Madelung potential of the oxide.^[18] Decreasing the Madelung potential results in a stronger basicity and larger polarization effects are induced on the adsorbed alkali atoms which are responsible for the reduction in the hfcc. In the case of the CRC, at which the electron is strongly polarized towards the low-coordinated cations (see Figure 5), the reduction in the Madelung potential moving down the alkaline earth oxide series should lead to the opposite effect, reducing the capability of the oxide cations to “strip” the unpaired electron spin density away from the parent nucleus.

Table 7. Computed properties of alkali atoms adsorbed on CRC sites of the $\text{MgO}(100)$ surface.^[a]

M	D_e [eV]	$r(\text{M}-\text{O})$ [Å]	$a_{\text{iso}}(M_{\text{ad}})$ [G] ^[b]	B_1 [G]	B_2 [G]	B_3 [G]	g_{xx}	g_{yy}	g_{zz}	$a_{\text{iso}}(^{17}\text{O})$ [G] ^[c]	$a_{\text{iso}}(^{25}\text{Mg})$ [G]
H ^[d]	1.75	0.98	-3.5 (1%)	6.0	-3.9	-2.1	2.00030	2.00040	2.00133	-28.5	-33.0
Li	1.64	1.84	26.3 (17%)	1.4	-0.8	-0.6	2.00049	2.00110	2.00160	-12.7	-11.3
Na	0.79	2.25	148.3 (44%)	2.3	-1.2	-1.0	1.99922	2.00052	2.00124	-18.0	-4.7
K	0.60	2.59	44.5 (53%)	0.4	-0.3	-0.1	1.99837	2.00027	2.00094	-13.8	-6.5

[a] D_e = adsorption energy; $r(\text{M}-\text{O})$ = shortest M–O distance. [b] The ratio with respect to the free-atom value is given in parentheses. [c] A partial spin density is found on the O_{4c} atom to which the alkali metal is bound. [d] From ref. [13] (EPR-II basis set on the hydrogen atom).

Assignment of adsorption sites of lithium, sodium, and potassium atoms on MgO: From the previous discussions it is clear that alkali metal atoms can bind to a variety of sites on the MgO surface, and that a combined use of theory and experiment can provide valuable information about the specific location of the atoms. As already mentioned, the population of a given site is directly correlated to the deposition temperature. In this section we try to summarize the information available to draw a unified picture.

For lithium atoms the situation is unambiguous. By analyzing the orientation of the g tensor with respect to the surface from angular-dependent measurements it can be directly shown that the EPR signal arises from lithium atoms adsorbed on terrace sites.^[7] This is conceivable in light of the calculated binding energy because the experiments were performed at a very low temperature. This result ties in well with the calculations of the g values and hfccs that show the best correlation with the terrace sites. From this direct comparison between theory and experiment one can safely conclude that the strategy to calculate and compare the EPR properties of alkali metals is perfectly suited to making predictions about the adsorption site, here an O_{5c} anion on a MgO(100) terrace. Note that it is expected that lithium atoms will also diffuse to low-coordinated sites, such as edges and corners, because of the diffusion of lithium atoms directly after deposition. For the relatively large amount of lithium (≈ 0.1 monolayer), which gives rise to the largest lithium atom EPR signal, small lithium metal clusters are expected on these low-coordinated sites. These clusters will, when they are paramagnetic, have a completely different EPR signal than single metal atoms.^[19,20] The experimentally observed EPR signal intensity of lithium atoms on terrace sites is markedly smaller than expected based on the amount of lithium deposited.^[7] Thus, this result can serve as indirect evidence for the formation of lithium clusters.

For potassium, there is ample evidence that adsorption occurs at the anionic reverse corner site.^[2] Herein the experiments were performed with high-surface-area polycrystalline samples in which the number of these sites is sufficiently large. The computed binding energy of potassium at this site suggests a higher barrier to diffusion, which is consistent with the thermal stability at room temperature. There are no other sites (except the CRC) to which potassium binds so strongly. On the other hand, HYSORE experiments^[2] have clearly shown that the potassium atoms interact simultaneously with three oxide anions on the surface, a condition which is fulfilled at an ARC site (and not at a CRC site). Finally, the computed g values are consistent with the measured ones and the theoretical $a_{\text{iso}}(\text{K})$ and $a_{\text{iso}}(\text{O})$ values are sufficiently close to the experimental ones. A direct comparison between theory and experiment for rubidium and cesium is not possible because the calculations herein have been carried out by using a pseudopotential to represent the atomic cores and thus the hfccs are not available. However, the tendency to bind heavier members of the series more weakly is confirmed, and the ARC is probably also the preferred adsorption site for these two atoms.

The case of sodium is more delicate. Sodium has an interaction strength with MgO intermediate between that of lithium (strong) and potassium (weak). As such, there are a few stable adsorption sites for sodium atoms: edge sites, reverse edges, and cationic and anionic reverse corners. On all of these sites the binding energy of sodium is between 0.6 and 1.5 eV. Comparison of the computed and measured g values is of little help here: All computed values are between 1.999 and 2.002, thus in the same range as the experimental values (2.000–2.001). The adsorption site has to be identified solely on the basis of the hfccs. The edge sites can be excluded because $a_{\text{iso}}(\text{Na})$ is too large (194 vs. 141 G) and, more importantly, the $a_{\text{iso}}(\text{O})$ is also too large (22 G, whereas it is only 2 G in the experiment). For the ARC site, $a_{\text{iso}}(\text{Na})$ is too small (93 G) and $a_{\text{iso}}(\text{O})$ is a bit too large (12 G). The two sites that provide the best agreement are thus the reverse edge ($a_{\text{iso}}(\text{Na})=169$ G and $a_{\text{iso}}(\text{O})=8$ G) and the CRC ($a_{\text{iso}}(\text{Na})=148$ G and $a_{\text{iso}}(\text{O})=18$ G). On this basis it is not possible to conclude unambiguously which is the most populated site. However, experiments performed on the more basic CaO and SrO indicate that the reverse edges are the most likely sites.^[3]

Conclusion

In the previous paragraphs we have presented the adsorption and EPR properties of hydrogen and alkali metal atoms deposited on various sites of the MgO surface. We have seen that they behave rather differently, and that hydrogen has a distinctly different reactivity compared with the alkali metal atoms.

By interacting with MgO, the hydrogen atom becomes ionized and forms a proton, which tightly bonds to an oxygen anion, and an electron, which remains trapped at specific morphological sites on the surface.^[9,10,13,14] These pairs of protons and trapped electrons, $(\text{H}^+)(\text{e}^-)$ ion pairs, are very important species responsible for the color of the sample and for its high chemical reactivity.^[14] As a consequence of this dissociation, no spin density is left on the adsorbed hydrogen. In contrast, a substantial spin density is always present on the adsorbed alkali metal atoms; the calculations indicate that the spin population is close to one (the only exception is with the CRC in which partial electron transfer occurs because of the particular conformation of the adsorption site). The electron spin density is strongly polarized, but the unpaired electron still resides on the alkali metal, in contrast to hydrogen.^[9] The reason for this different behavior is the special character of the proton. In both cases, hydrogen and alkali metals, the ionization of the adatom occurs if the cost of ionization is overcompensated by the formation of a sufficiently strong $\text{O}-\text{M}^+$ bond ($\text{M}=\text{H}, \text{Li}, \text{etc.}$). Hydrogen has a very high ionization potential (13.6 eV), but the proton affinity of the oxide anions is also very high (of the order of 10–12 eV). If the electron is stabilized at other morphological sites on the surface, the result is an energetically favorable process and a stable $(\text{H}^+)(\text{e}^-)$

ion pair. The situation is quite different for the alkali metal atoms. Here the ionization potential ranges from 5.4 (Li) to 3.9 eV (Cs). In this respect, the cost of forming a positively charged species is much less than in the case of hydrogen. However, the corresponding energy gain obtained by binding the alkali metal cation to the MgO surface is much smaller and depends critically on the adsorption site.

Different sites clearly present different bonding capabilities. This also represents a potential for the use of alkali metal atoms as “atomic probes” to test and monitor the surface morphology and basicity.^[2,3] In this respect, it is very important to know at which temperature the experiments are carried out. Low-coordinated sites, like steps, edges, kinks, corners, and reverse corners, are minority sites with respect to the flat (100) terraces. Of course, the number of irregular sites varies with the preparation method and with the surface area of the sample. Nevertheless, even for highly irregular and morphologically complex surfaces, the flat terraces are dominant. Alkali metal atoms deposited at low temperatures have a higher probability of nucleating on flat terraces after dissipating their excess energy to the surface. Thus, in low-temperature experiments it is expected that terrace sites will be decorated with alkali adatoms. This is indeed the case with lithium deposited on MgO thin films. However, if the thermal energy is sufficient to overcome the relatively low barrier to diffusion, the atoms will move freely across the surface and have the time and the energy to explore large portions of the surface. Thus, adsorption on regular terrace sites occurs only at very low temperatures for all the alkali metal atoms considered: The diffusion barriers on MgO(100) estimated from DFT calculations are <0.4 (Li), <0.2 (Na), and <0.1 eV (K). Experimentally it has been shown that annealing to 70 K is sufficient to induce the diffusion of lithium atoms across the MgO(100) terraces until they become trapped at particularly strong binding sites, like the low-coordinated atoms or other defects.^[7]

The experiments on the polycrystalline MgO samples were performed at room temperature. The fact that the atomic species are clearly visible and that no aggregation or formation of metal particles is observed for low coverage of alkali metals is a sign of the relatively strong bonding between the alkali metal atoms and the surface sites. A thermally stable sample at about 300 K corresponds to a binding energy of the metal atom of about 0.8 eV (determined by using the Redhead equation with a frequency factor of 10^{13} s^{-1}). This condition is met when the alkali atom is bound to special sites, such as the anionic reverse corner formed at the intersection of two steps. This particular site has been identified as the most likely binding site for potassium on polycrystalline MgO.^[2] The results and discussion presented herein have shown that the situation may be more difficult for atoms, such as sodium, for which the oxygen reverse edge has been found to be the most likely adsorption site.

Experimental Section

Sample preparation: Most of the experiments were performed in a vacuum (residual pressure 10^{-5} mbar) with polycrystalline MgO as the support. The metals considered were sodium, potassium, rubidium, and cesium. Attempts to deposit lithium on polycrystalline MgO led to single unresolved EPR resonances and no monomeric species could be detected. High surface area polycrystalline MgO was prepared by slow decomposition of the corresponding hydroxides as described elsewhere.^[21] Thermal activation at 1173 K produces virtually hydroxy-free samples.^[22,23]

In the case of sodium, potassium, and rubidium, metal shots were distilled in a vacuum to form a metal mirror in a separate part of the quartz cell used for EPR measurements. The cesium metallic mirror was formed by the thermal decomposition of CsN_3 . The metal was evaporated on the sample in situ by heating the metallic mirror while keeping the powder at nearly room temperature. The amount of metal deposited on the sample was roughly controlled by varying the exposure time of the powder to the metal vapors. EPR spectra were recorded at 298 and 77 K by using a Bruker EMX spectrometer operating at X-band frequencies and equipped with a cylindrical cavity operating at a field modulation of 100 kHz. Continuous wave (CW) spectra were recorded at 1 mW microwave power and 0.5 G modulation amplitude. The CW-EPR spectra were simulated by using the Easyspin package.^[24]

Lithium atoms were deposited at 35 K on a 20 monolayer thick MgO-(001) film grown on a Mo(001) substrate.^[7] The amount of lithium was calibrated by a quartz microbalance. The films were prepared by reactive deposition of magnesium in an oxygen atmosphere of 1×10^{-6} mbar. The MgO film was annealed to 1100 K for 10 min. The EPR spectra of the lithium atoms were measured at 35 K with a Bruker EMX spectrometer operating at X-band frequencies and equipped with a TE₁₀₂ cavity operating at a 100 kHz field modulation. Unless stated otherwise a microwave power of 2 mW and a modulation amplitude of 4 G were used.^[7]

DFT calculations: The surface of MgO is represented by a finite nano-cluster containing a few thousand atoms. The central part of the cluster, treated quantum mechanically, is surrounded by about 700–800 classical ions whose polarizability is described by a shell model (SM).^[25] Cations in the SM region at the interface with the quantum mechanical (QM) region are replaced by ions (hereafter indicated as Mg*) on which a semi-local effective pseudopotential (ECP) is centered, to reproduce the Pauli repulsion and avoid the nonphysical polarization of QM interface anions. Region I, the QM and SM region, is then surrounded by a large array of about 3000 point charges (PC) to reproduce the long-range electrostatic potential.

This scheme is implemented in the GUESS code^[26] interfaced with the Gaussian 03 code,^[27] and the total energy of the hybrid system is calculated as the sum of the classical and QM contributions. Forces acting on all the centers in region I, both QM and classical (cores and shells), can be calculated to allow the simultaneous optimization of their position. All centers in the QM region and the Mg* interface atoms were allowed to move during the optimization, whereas only shells, not cores, were relaxed in the SM region. Thus, the electronic polarization was included in a large portion of the surface, whereas ionic polarization is restricted to a few tens of atoms. The total energy and the electronic structure of the QM cluster were calculated by DFT calculations by using the hybrid B3LYP exchange-correlation functional.^[28,29]

The following QM clusters have been considered to model various sites on the MgO surface: $\text{Mg}_9\text{O}_9\text{Mg}^*_{16}$ (terrace), $\text{Mg}_{10}\text{O}_{10}\text{Mg}^*_{14}$ (edge), $\text{Mg}_{18}\text{O}_{18}\text{Mg}^*_{30}$ (reverse edge), $\text{Mg}_{11}\text{O}_{11}\text{Mg}^*_{18}$ (anionic reverse corner), and $\text{Mg}_{17}\text{O}_{17}\text{Mg}^*_{24}$ (CRC). The 6-311+G** basis set was used for hydrogen atoms adsorbed on terrace sites; the 6-311+G* basis set was used for lithium, sodium, and potassium. Rubidium and cesium atoms were treated with a lanl2 ECP (small core) and a lanl2dz basis set. The magnesium and oxygen nearest neighbors of the adsorbate were treated with a 6-31G* basis set, the rest with a standard 6-31G basis set. The adsorption energies were not corrected for the basis set superposition error, but this was expected to be small (about 0.1 eV) given the large basis set used for the alkali atoms.

To estimate the spatial distribution of the unpaired electron in paramagnetic centers, atomic spin populations were evaluated and plots of iso-surfaces at constant spin density were generated. For the EPR properties of the paramagnetic adatoms we considered both the isotropic and dipolar parts of the hyperfine coupling matrix (expressed in gauss) of the alkali metals, the ^{25}Mg and ^{17}O nuclides, and the g factors. As the evaluation of the hfccs required full treatment of the atomic cores (all electron calculations) the analysis was restricted to lithium, sodium, and potassium atoms.

The rather complex description of g values in terms of electronic structure parameters requires the consideration of various magnetic contributions^[30] and the use of sufficiently accurate eigenfunctions. The spin-orbit interaction, which is crucial for quantifying the deviation of g from the free-electron value g_e ^[30] could be either accounted for self-consistently or treated as a perturbation. Herein we used the spin-orbit perturbation strategy in the scheme proposed by Neese^[31] and implemented in the Gaussian 03 code adopted for all the calculations.^[27]

EPR spectra: The interaction of alkali metal atoms with dehydrated, high-surface-area, polycrystalline MgO leads to EPR spectra characteristic of isolated monomeric species.^[2,3] Figure 6 shows representative X-band EPR spectra recorded at 77 K obtained from sodium and cesium vapors in contact with a dehydrated MgO sample, activated at 1173 K.

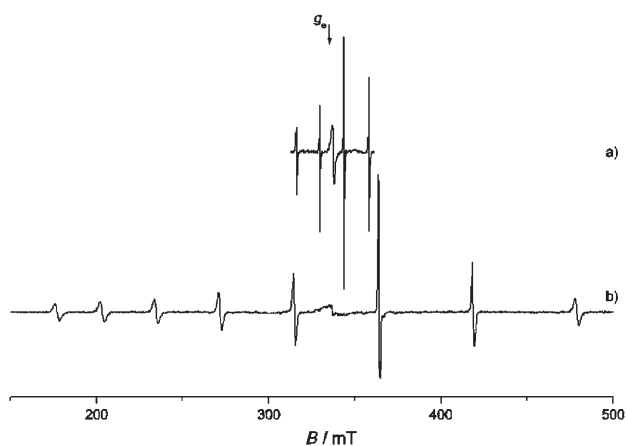


Figure 6. EPR spectra recorded of a) sodium atoms and b) cesium atoms adsorbed on the surface of polycrystalline MgO at 77 K.

Let us consider first the sodium spectrum. This is dominated by a quartet of lines separated by about 140 G (14 mT), which arise from the hyperfine interaction of the unpaired electron spin with the nuclear spin of the sodium atom ($I=3/2$). Similar results were obtained for the deposition of potassium atoms and a detailed analysis of the signal can be found in references [2] and [3]. A small unresolved signal is present in the experimental spectrum at approximately $g=2$. This signal contains contributions from ionized alkali cations (<1%) that result from the adsorption on tiny amounts of surface oxygen vacancies (F centers)^[4] or nearby residual surface OH⁻ groups,^[32] which are both capable of inducing spontaneous ionization of the metal. Contributions from small metal particles also leads to resonance absorption in the same region.^[5]

A full account of the results obtained for cesium is given in the Supporting Information.

Acknowledgements

This work was supported by the Italian MIUR through a Cofin 2005 project and by the European COST action D41 "Inorganic oxide surfaces and interfaces". E.G. would like to thank the Alexander von Humboldt

Foundation for support. J.L., T.R., and H.J.F. also acknowledge support from the Cluster of Excellence "Unifying Concepts in Catalysis" coordinated by the Technische Universität Berlin and funded by the Deutsche Forschungsgemeinschaft.

- [1] J. H. Lunsford, *Angew. Chem.* **1995**, *107*, 1059; *Angew. Chem. Int. Ed. Engl.* **1995**, *34*, 970.
- [2] M. Chiesa, E. Giamello, C. Di Valentin, G. Pacchioni, Z. Sojka, S. Van Doorslaer, *J. Am. Chem. Soc.* **2005**, *127*, 16935.
- [3] M. Chiesa, F. Napoli, E. Giamello, *J. Phys. Chem. C* **2007**, *111*, 5481.
- [4] S. Brazzelli, C. Di Valentin, G. Pacchioni, E. Giamello, M. Chiesa, *J. Phys. Chem. B* **2003**, *107*, 8498.
- [5] D. M. Murphy, E. Giamello, *J. Phys. Chem.* **1995**, *99*, 15172.
- [6] F. Hensel, P. P. Edwards, *Chem. Eur. J.* **2006**, *2*, 1201.
- [7] J. C. Lian, E. Finazzi, C. Di Valentin, H.-J. Gao, T. Risse, G. Pacchioni, H.-J. Freund, *Chem. Phys. Lett.* **2008**, *450*, 308.
- [8] E. Giamello, M. C. Paganini, D. M. Murphy, A. M. Ferrari, G. Pacchioni, *J. Phys. Chem. B* **1997**, *101*, 971.
- [9] D. Ricci, C. Di Valentin, G. Pacchioni, P. V. Sushko, A. L. Shluger, E. Giamello, *J. Am. Chem. Soc.* **2003**, *125*, 738.
- [10] M. Chiesa, M. C. Paganini, E. Giamello, C. Di Valentin, G. Pacchioni, *Angew. Chem.* **2003**, *115*, 1801–1803; *Angew. Chem. Int. Ed.* **2003**, *42*, 1759.
- [11] M. Chiesa, M. C. Paganini, E. Giamello, C. Di Valentin, G. Pacchioni, *ChemPhysChem* **2006**, *7*, 728.
- [12] M. Sterrer, T. Berger, O. Diwald, E. Knözinger, *J. Am. Chem. Soc.* **2003**, *125*, 195.
- [13] M. Chiesa, M. C. Paganini, G. Spoto, E. Giamello, C. Di Valentin, A. Del Vitto, G. Pacchioni, *J. Phys. Chem. B* **2005**, *109*, 7314.
- [14] M. Chiesa, M. C. Paganini, E. Giamello, D. M. Murphy, C. Di Valentin, G. Pacchioni, *Acc. Chem. Res.* **2006**, *39*, 861.
- [15] M. Yulikov, M. Sterrer, M. Heyde, H.-P. Rust, T. Risse, H. J. Freund, G. Pacchioni, A. Scagnelli, *Phys. Rev. Lett.* **2006**, *96*, 146804.
- [16] M. Chiesa, E. Giamello, G. Annino, C. A. Massa, D. M. Murphy, *Chem. Phys. Lett.* **2007**, *438*, 285.
- [17] A. Bondi, *J. Phys. Chem.* **1964**, *68*, 441.
- [18] G. Pacchioni, J. M. Ricart, F. Illas, *J. Am. Chem. Soc.* **1994**, *116*, 10152.
- [19] A. D. Garland, D. M. Lindsay, *J. Chem. Phys.* **1984**, *80*, 4761.
- [20] D. Murphy, E. Giamello, A. Zecchina, *J. Phys. Chem.* **1993**, *97*, 1739.
- [21] I. Purnell, M. Chiesa, R. D. Farley, D. M. Murphy, C. C. Rowlands, M. C. Paganini, E. Giamello, *Magn. Reson. Chem.* **2002**, *40*, 381.
- [22] C. Chizallet, G. Costentin, M. Che, F. Delbecq, P. Sautet, *J. Phys. Chem. B* **2006**, *110*, 15878.
- [23] C. Chizallet, G. Costentin, M. Che, F. Delbecq, P. Sautet, *J. Am. Chem. Soc.* **2007**, *129*, 6442.
- [24] S. Stoll, A. Schweiger, *J. Magn. Reson.* **2006**, *178*, 42.
- [25] B. G. Dick, A. Overhauser, *Phys. Rev.* **1958**, *112*, 90.
- [26] P. V. Sushko, A. L. Shluger, C. R. A. Catlow, *Surf. Sci.* **2000**, *450*, 153.
- [27] Gaussian 03, Revision A.07, M. J. Frisch, G. W. Trucks, H. B. Schlegel, G. E. Scuseria, M. A. Robb, J. R. Cheeseman, J. A. Montgomery, Jr., T. Vreven, K. N. Kudin, J. C. Burant, J. M. Millam, S. S. Iyengar, J. Tomasi, V. Barone, B. Mennucci, M. Cossi, G. Scalmani, N. Rega, G. A. Petersson, H. Nakatsuji, M. Hada, M. Ehara, K. Toyota, R. Fukuda, J. Hasegawa, M. Ishida, T. Nakajima, Y. Honda, O. Kitao, H. Nakai, M. Klene, X. Li, J. E. Knox, H. P. Hratchian, J. B. Cross, V. Bakken, C. Adamo, J. Jaramillo, R. Gomperts, R. E. Stratmann, O. Yazyev, A. J. Austin, R. Cammi, C. Pomelli, J. W. Ochterski, P. Y. Ayala, K. Morokuma, G. A. Voth, P. Salvador, J. J. Dannenberg, V. G. Zakrzewski, S. Dapprich, A. D. Daniels, M. C. Strain, O. Farkas, D. K. Malick, A. D. Rabuck, K. Raghavachari, J. B. Foresman, J. V. Ortiz, Q. Cui, A. G. Baboul, S. Clifford, J. Cioslowski, B. B. Stefanov, G. Liu, A. Liashenko, P. Piskorz, I. Komaromi, R. L. Martin, D. J. Fox, T. Keith, M. A. Al-Laham, C. Y. Peng, A. Nanayakkara, M. Challacombe, P. M. W. Gill, B. Johnson, W. Chen, M. W. Wong, C. Gonzalez, J. A. Pople, Gaussian, Inc., Wallingford CT, **2004**.

- [28] A. D. Becke, *J. Chem. Phys.* **1993**, *98*, 5548.
[29] C. Lee, W. Yang, R. G. Parr, *Phys. Rev. B* **1998**, *37*, 785.
[30] J. E. Harriman, *Theoretical Foundations of Electron Spin Resonance*, Academic Press, New York, **1978**.
[31] F. Neese, *J. Chem. Phys.* **2001**, *115*, 11080.
[32] F. Napoli, M. Chiesa, E. Giamello, E. Finazzi, C. Di Valentin, G. Pacchioni, *J. Am. Chem. Soc.* **2007**, *129*, 10575.

Received: December 20, 2007
Published online: March 26, 2008